Nonempirical Analysis of Nature of Catalytic Effects in Ribonuclease A Active Site

PAWEŁ KĘDZIERSKI,[1] W. ANDRZEJ SOKALSKI,[1] MORRIS KRAUSS[2]

[1]*Institute of Physical and Theoretical Chemistry, Wrocław University of Technology, Wyb. Wyspiańskiego 27, 50-370 Wrocław, Poland*

[2]*Center for Advanced Research in Biotechnology, National Institute of Standards and Technology, 9600 Gudelsky Drive, Rockville, Maryland 20850*

Received 26 July 1999; accepted 9 November 1999

ABSTRACT: The physical nature of the catalytic activity exerted by various ribonuclease A active site constituents is analyzed in terms of the differential transition state stabilization approach in which activation barrier changes induced by the molecular environment are expressed by additive components defined in the theory of intermolecular interactions. Electrostatic multipole contributions seem to approximate total catalytic activity well for residues separated by contacts longer than 2.7 Å whereas at shorter distances the remaining exchange and delocalization terms are not negligible. Depending on the reaction step, the same residue may exhibit catalytic or inhibitory activity.
 J Comput Chem 21: 432–445, 2000

Keywords: ribonuclease A; catalytic activity; electrostatic effects; intermolecular interactions; active site

Introduction

Currently, the most reliable models of reaction mechanisms and the nature of catalytic effects in enzymes can be obtained by means of nonempirical calculations. Models of large reactants involved in biological systems often require numerous assumptions concerning the starting point for such expensive calculations. A common example is the different protonation states for the model mimicking the active site of an enzyme. Because the number of possible variants makes more rigorous and systematic calculations impossible, such decisions are made on the basis of chemical intuition, which is supported with experimental and theoretical pK_a or by means of empirical modeling. This area of research needs semiquantitative tools, which may be used to test hypothetical reaction variants to rule out the less relevant ones. The physical na-

Correspondence to: W. A. Sokalski; e-mail: sokalski@mml.ch.pwr.wroc.pl

Contract/grant sponsor: NIST; contract/grant number: 43NANB614782

Contract/grant sponsor: KBN; contract/grant number: 6 PO4A 060 09

ture of catalytic activity may be analyzed within the differential transition state stabilization model[1] in which the activation barrier lowering that is due to the catalytic environment is directly expressed by additive components defined in terms of intermolecular interaction theory. This allows the extraction of the most essential components contributing to catalytic activity and the derivation of simpler theoretical models in a rational way. Until recently most of the nonempirical studies of enzymatic systems employed the supermolecular approach in which the analysis of the physical nature of catalytic activity was not possible. In simpler models, which are most frequently based on empirical force fields, corresponding terms had no clear defined physical meaning. Nevertheless, previous empirical or semiempirical studies mostly indicated the dominant role of electrostatic effects in enzymatic catalysis.[1–6] However, the absolute magnitude of the nonelectrostatic contributions to catalytic activity has not as yet been determined from precise nonempirical calculations. This implies a need for quantitative research on electrostatic and nonelectrostatic contributions to enzymatic catalysis to provide a basis for more reliable approximations in defining the model systems. Solving this problem requires efficient *ab initio* energy decomposition of the interaction energies capable of treating relatively large fragments of the enzyme active site.

Various perturbational or variational decompositions of intermolecular interaction energies have been developed.[7–14] They usually identify first-order electrostatic and exchange contributions, but the higher order terms differ in definition. Until recently, applications of these methods were limited to systems no larger than 100–200 atomic orbitals because of the huge amount of disk space required for evaluation or transformation of two-electron integrals.[15] In the present work we employ a hybrid variation–perturbation self-consistent field (SCF) interaction energy decomposition scheme[12] using a DIRECT algorithm. Current implementation of this approach can be used to study systems of up to 600 basis functions, which opens the way to study medium-sized models of enzymatic reactions.

As the test case, we selected a reaction performed by bovine pancreatic ribonuclease A (RNAse A, EC 3.1.27.5). This enzyme has been extensively studied experimentally and theoretically. For example, over 70 structures related to RNAse A are available from the Protein Data Bank. Despite the extensive pool of experimental data, the details of the reaction performed by this enzyme are still the subject of interest and controversy. This is typical for enzymes, where the reaction center comprises a number of active residues and their role cannot be evaluated independently. The initial theoretical studies on RNAse A, which focused on the interactions between the substrate and residues as a function of protonation state,[16–20] provided an insight into the initial substrate interactions, but they could not characterize the intermediates and transition states that lie along the enzyme-catalyzed reaction pathway. The remaining studies can be divided by whether they use empirical[21–23] or *ab initio*[24–26] methods to calculate the reaction path. The conclusions diverge on details of the mechanism and are hard to compare because of differences in the methods used and, perhaps even more significantly, the active site model of the transition state complex.

In this work we analyze the interactions within the active site for the initial stages proceeding in the ribonuclease A active site, and we attempt to evaluate the catalytic roles played by various active site residues within the active site environment. Our aims are the following:

- to evaluate from first principles the physical nature of catalytic activity of various active site residues at different stages of the transphosphorylation reaction;
- to analyze the distance dependence of various terms of interaction energy in order to recognize the boundaries, where different physical contributions must be taken into account;
- to examine the role of the electrostatic term in the catalytic activity in order to verify the assumption on the dominant role of the electrostatic contribution to stabilization of transition states;
- to test various approximate models of the electrostatic term with the exact values; and
- to determine the effect that an accurate description of the electrostatics could have on the determination of the protonation states of the catalytic residues and on their roles in the reaction mechanism, relative to earlier conclusions.

Reaction Catalyzed by RNAse A

RNAse A is a 124 residue form of a digestive enzyme predominant in secretory cells of bovine pancreas. RNAse A performs two subsequent reactions that cleave the RNA strand leaving the 3′ PO_4 and 5′ OH group. The first step is a transphosphorylation leading to breakage of the P—$O^{5'}$ bond and creation

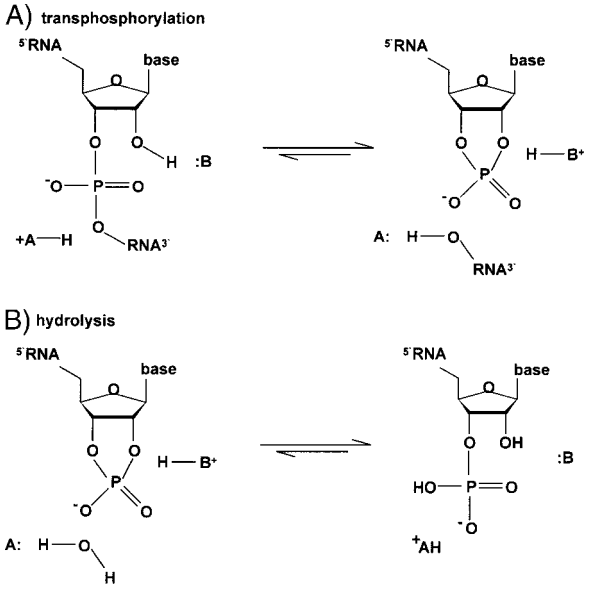

FIGURE 1. A schematic presentation of the generalized reaction mechanisms catalyzed by ribonuclease A. A, general acid; B, general base.

of a cyclic phosphodiester (Fig. 1a). In the second step this cyclic phosphodiester is hydrolyzed (Fig. 1b). Raines recently reviewed the experimental behavior.[27] The active site residues that were shown to be involved in the mechanism include Gln 11, His 12, Lys 41, His 119, Phe 120, and Asp 121. It is generally believed that RNAse A acts as a general acid–general base catalyst (Fig. 1); the general acid is believed to be His 119 and the general base His 12. Within this assumption, experimental and theoretical mechanisms have both been suggested.[23, 24, 28–30] However, the other active site residues, namely, Lys 41 and the phosphate itself, can act as bases under the desolvated conditions in the active site.[31] A detailed *ab initio* calculation of the reaction path by Wladkowski et al.[25, 26] supports the active involvement of the phosphate and also suggests an active role for Lys 41. Two alternative reaction paths obtained in this theoretical study were supplemented with calculations that took into account the electron correlation [on second-order Möller–Plesset (MP2) and density functional theory (DFT) levels] and the incorporation in the quantum Hamiltonian of residues that are not chemically involved by representing them with effective fragment potentials (EFPs).[32] In addition, we also tested whether some of the stationary points proposed earlier[26] require the use of a single- or multideterminant wavefunction, using a Monte Carlo SCF (MCSCF) approach.[33] Although the electron correlation has a substantial effect on the activation energies calculated at the SCF level, the electronic characteristics of the SCF are sufficiently accurate to use the stationary point structures from ref. 26 as the basis for the present analysis.

Methods

In order to quantitatively represent the influence of active site residues on the activation barrier, we used the differential transition state stabilization approach,[1] which is related to the Pauling concept[34] in which the activation energy change $\Delta\Delta E_{\mathrm{res}}$ resulting from the presence of an active site residue (res) is written as

$$\Delta\Delta E_{\mathrm{res}} = \Delta E_{\mathrm{TS,res}} - \Delta E_{\mathrm{SC,res}} \tag{1}$$

where $\Delta E_{\mathrm{TS,res}}$, $\Delta E_{\mathrm{SC,res}}$ represent counterpoise corrected interaction energies between reactants (TS, the transition state; SC, the substrate complex) and active site residues. Both the SCF interaction energies of TS,res and SC,res were decomposed into the first-order electrostatic, first-order exchange, and higher order delocalization components calculated in the dimer basis set (D):

$$\Delta E^{\mathrm{SCF}}(D) = E^{(1)}_{\mathrm{el}}(D) + E^{(1)}_{\mathrm{ex}}(D) + E^{(\mathrm{R})}_{\mathrm{del}}(D). \tag{2}$$

The sum of first-order terms is the zeroth-iteration interaction energy, where the initial density matrix was formed from mutually orthogonal eigenvectors of isolated A and B molecules calculated in the dimer basis set. The electrostatic term is then obtained within a perturbational framework using the expression

$$\begin{aligned} E^{(1)}_{\mathrm{el}}(D) = &\sum_r\sum_s\sum_t\sum_u P^{\mathrm{A}}_{rs}(D)P^{\mathrm{B}}_{tu}(D)\langle rs|R_{12}^{-1}|tu\rangle \\ &+ \sum_r\sum_s\sum_b P^{\mathrm{A}}_{rs}(D)\langle r|-Z_bR_{1b}^{-1}|s\rangle \\ &+ \sum_t\sum_u\sum_a P^{\mathrm{B}}_{tu}(D)\langle t|-Z_aR_{1a}^{-1}|u\rangle \\ &+ \sum_a\sum_b Z_aZ_bR_{ab}^{-1}. \end{aligned} \tag{3}$$

The exchange term is then calculated as the difference of first-order interaction energy and the electrostatic term

$$E^{(1)}_{\mathrm{ex}}(D) = E^{(1)}(D) - E^{(1)}_{\mathrm{el}}(D). \tag{4}$$

This hybrid variation–perturbation decomposition procedure[12] has several advantages over other schemes that can be found in the literature.[7–10] It uses counterpoise correction for basis set superposition error consistently for all terms and this accounts

for the considerably reduced basis set dependence of its components.[12] The procedure is also relatively inexpensive when compared to other, mostly perturbational approaches involving additional time consuming integral transformation. Therefore, it seems well suited to use for relatively large systems of biological interest.

Using this scheme, the SCF energy changes $\Delta\Delta E_{\mathrm{res}}$ resulting from the presence of active site residues may be decomposed into the following physical components:

$$\Delta\Delta E_{\mathrm{res}}^{\mathrm{SCF}} = \Delta E_{\mathrm{el}}^{(1)}(\mathrm{res}) + \Delta E_{\mathrm{ex}}^{(1)}(\mathrm{res}) + \Delta E_{\mathrm{del}}^{(\mathrm{R})}(\mathrm{res}), \quad (5)$$

where $\Delta E_{\mathrm{el}}^{(1)}(\mathrm{res}) = E_{\mathrm{el}}^{(1)}(\mathrm{TS,res}) - E_{\mathrm{el}}^{(1)}(\mathrm{SC,res})$ etc.

The electrostatic term $E_{\mathrm{el}}{}^{(1)}$ was also approximated within an exponent truncated cumulative atomic multipole moment (CAMM) expansion[35] using atomic multipoles generated from the monomer (TS, res, or SC) wave functions:

$$\Delta E_{\mathrm{el,CAMM}}^{(1)} = E_{\mathrm{el,CAMM}}^{(1)}(\mathrm{TS,res}) - E_{\mathrm{el,CAMM}}^{(1)}(\mathrm{SC,res}). \quad (6)$$

In this work we used exponent truncated expansion of the CAMM series up to a monopole–octupole term, which reproduces about 97% of the electrostatic potential on the Connolly envelope.[36] The difference between $E_{\mathrm{el}}^{(1)}$ and $E_{\mathrm{el,CAMM}}^{(1)}$ converges with the expansion of the CAMM series to the penetration part of the electrostatic energy. In this way we were also able to examine the error introduced by the neglect of penetration energy, which is the case in most electrostatic models of interactions.

In order to check the electronic state of the system, one of the alternative pathways, namely R2 ⇒ PTTS3 (see below), was also analyzed on the MCSCF level[33] using the active space of three occupied and three virtual orbitals. These calculations revealed more than 95% of the singlet character of the stationary points, which supports the validity of the single-determinant restricted Hartree–Fock (RHF) energy surface in this case.

All calculations were carried out with the standard 6-31G** split-valence basis set using the Gaussian 94[37] and GAMESS packages.[38] The decomposition scheme was implemented in GAMESS code using the direct SCF algorithm.[38]

Model of RNAse A Active Site

The model of the RNAse A active site proposed by Wladkowski et al.[25,26] seems to be the most complete and up to date. The actual substrate was mimicked by the 2-hydroxyethyl methyl phosphate (HEMP) monoanion, which represents the smallest model with the essential features necessary to undergo intramolecular transphosphorylation. Three most important active site residues were represented by imidazole rings (His 12 and His 119) and by a methylamine molecule (Lys 41). To distinguish them from complete residues, these components of the active site model are labeled in this text as His 12*, His 119*, and Lys 41* (Fig. 2). The rest of the active sites (all residues within an 8 Å sphere) were represented by EFPs.[26] It must be noted that the EFP approach was used solely for verification of energies of stationary points on the system's potential energy surfaces, which were determined using the RHF method and 3-21+G(d) basis set. This model still does not include more distant enzyme atoms or the solvent; although they may have an impact on the catalysis, they should not influence the roles of catalytic residues, so the model seems sufficient for our analysis. The method is however by no means restricted to the first shell, and inclusion of the rest of the environment of importance could further improve the results involving structured dielectric effects.

Wladkowski et al.[25,26] considered two parallel pathways starting from different protonation states of the system (Fig. 3). This does not exhaust all the possible hypothetical protonation states; only for the case when one assumes the total charge of +1, there are 56 possibilities. However, it was not the aim of the present study to decide which state of protonation is the valid one. The number of alternatives is unacceptably large for systematic investigations on the nonempirical level and could only be addressed by either some kind of iterative (semi)empirical calculations or chemical intuition, which is supported by experimental data like the pK_a for amino acids in a particular environment. Both treatments would benefit from information on the specific roles of catalytic residues in interactions with the bound ligand. For our purposes, both of the well-defined (in terms of structures) parallel pathways (R1 ⇒ PTTS1 ⇒ I1 ⇒ PTTS2 and R2 ⇒ PTTS3) open the possibility of comparing the catalytic effect of the same residue in two different models.

Figure 3 shows the energy diagram for the overall reaction path as determined in ref. 26, and Figure 2 visualizes the structures of these species that we analyze in the present work. Within the framework of the differential transition state stabilization approach,[1] based on perturbation theory, reactant–ligand interaction energy is defined for rigid subunits only. Therefore, the present analysis is done for static structures. The boundaries of subunits can-

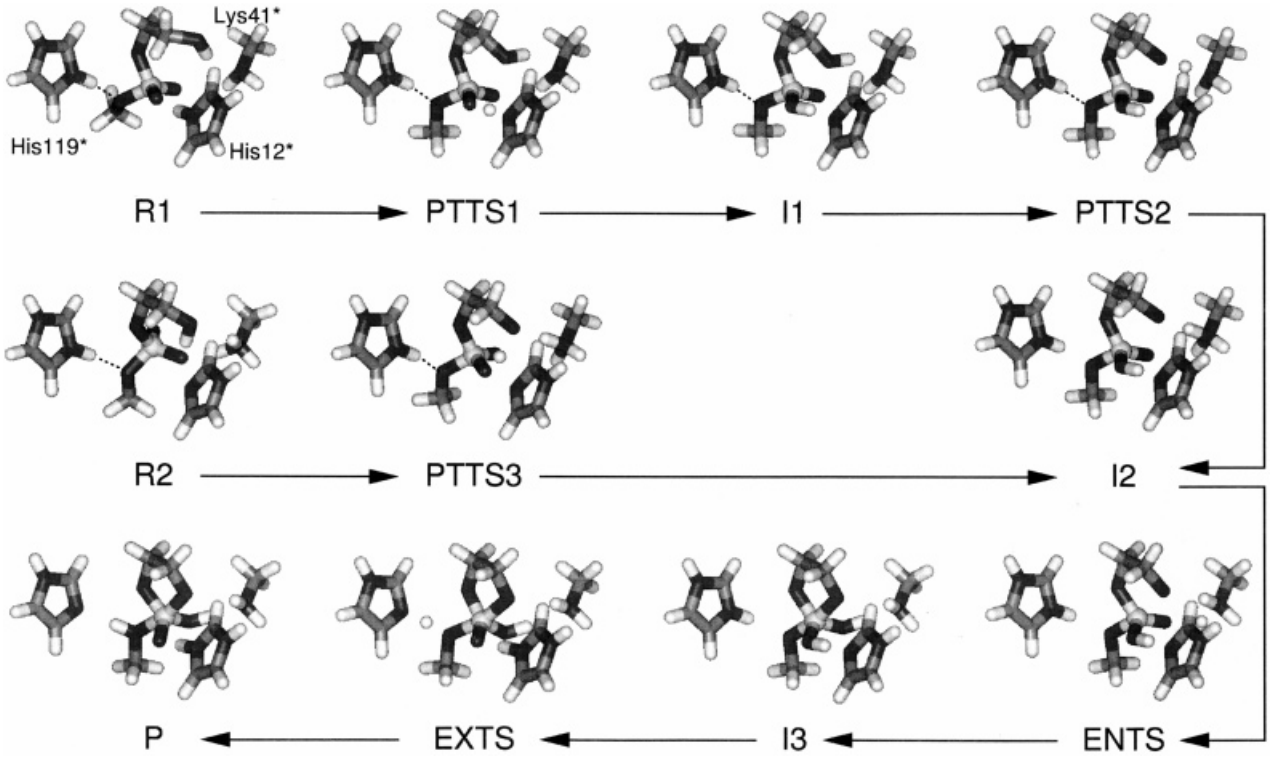

FIGURE 2. The two alternative pathways of the initial phase of transphosphorylation performed by RNAse A.[25, 26] In this scheme the roles of the active residues change along the pathway. In the mechanism starting from R1 the His 12 acts initially as an acid and Lys 41 as a base; in the alternative scheme (R2 → PTTS3) the phosphate group serves initially as the base. In the following common stages the His 119 becomes the general acid and His 12 the general base, which is consistent with earlier propositions.[27]

not be defined across the bonds being made (or broken) during a particular reaction step. This imposes the restriction that if one wants to compare the role played by a residue at different stages of reactions, the residue must not be involved in the reaction at any of these stages. Such is the case for the pathway going from R1 to PTTS2, where His 12* and Lys 41* participate in proton transfers to and from HEMP, so for this pathway we determined the role of His 119* only. For the R2 ⇒ PTTS3 step, the reactants constitute the HEMP molecule solely, where an intramolecular proton transfer takes place. For this case we could examine in detail catalytic effects of all of the three catalytic residues His 12*, His 119*, and Lys 41* (Tables I, II). Further stages of reaction were not investigated here because they do not involve alternative mechanisms and they are possibly less accurately determined, because the published HF, MP, and DFT results are substantially different.[26]

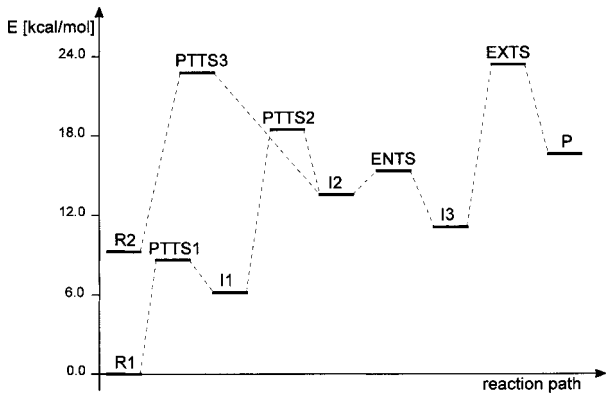

FIGURE 3. A relative energy diagram for the reaction models proposed by Wladkowski et al.[26] and presented in Figure 2.

Results and Discussion

The calculated components of interaction energies between various reactants and ligands are presented in Table I. At the equilibrium distances the value of every energy component constitutes a non-negligible portion of the interaction energy. In some

TABLE I.
Interaction Energies between Various Residues and Model Reactant Systems for Different Stages of Reaction (kcal/mol).

Interacting Species	$\Delta E_{res}^{SCF}(D)$	$E_{el}^{(1)}(D)$	$E_{ex}^{(1)}(D)$	$E_{del}^{(R)}(D)$	Shortest Distance (Å)
R1:H119δ*	−7.32	−18.67	18.25	−6.90	1.76
R1:H119+*	−33.07	−36.35	15.86	−12.58	1.76
PTTS1:H119δ*	−6.03	−18.09	19.06	−7.01	1.74
PTTS1:H119+*	−28.89	−32.67	16.51	−12.73	1.74
I1:H119δ*	−4.49	−16.13	17.74	−6.10	1.76
I1:H119+*	−24.36	−28.10	15.31	−11.57	1.76
PTTS2:H119δ*	−5.80	−15.71	15.50	−5.59	1.81
PTTS2:H119+*	−29.36	−31.74	13.37	−10.99	1.81
R2:H119δ*	−13.51	−14.81	4.92	−3.62	2.32
R2:H12+*	−70.91	−69.97	4.17	−5.11	2.36
R2:H12δ*	3.73	1.97	4.04	−2.28	2.36
R2:H12ε*	−9.43	−11.72	4.84	−2.56	2.36
PTTS3:H119δ*	−11.09	−18.02	12.94	−6.01	1.87
PTTS3:H12+*	−84.73	−85.32	9.97	−9.37	2.35
PTTS3:H12δ*	5.27	1.07	8.29	−4.10	2.35
PTTS3:H12ε*	−11.98	−17.39	10.60	−5.20	2.35

cases the electrostatic term alone seems to reproduce the total SCF energy well, but for short distances this is usually an accidental agreement and appears because of cancellation of the exchange and delocalization contributions.

Table II contains a detailed analysis of interactions of all residues composing the R2 and PTTS3 structures with the HEMP substrate undergoing intramolecular proton transfer (Fig. 2). The energies in Table II are differential stabilization energies of the PTTS3 form of HEMP relative to interaction energies with the R2 form, so they are directly interpretable as contributions to the lowering of the activation energy at this reaction step. Careful analysis of these numbers leads to the conclusion that at equilibrium distances none of the contributions can be safely neglected, except for the most catalytically active His 12* residue. Even for relatively strong interactions the common assumption on the predominant role of the electrostatic term

TABLE II.
Activation Energy Changes for First Reaction Stage (R2 ⇒ PTTS3) Resulting from Protonation of Active Site Residues (kcal/mol).

Environment (Res)	$\Delta\Delta E_{res}^{SCF}(D)$	$\Delta E_{el}^{(1)}(D)$	$\Delta E_{ex}^{(1)}(D)$	$\Delta E_{del}^{(R)}(D)$	$\Delta E_{el,CAMM}^{(1)}$
His 12+*	−13.81	−15.35	5.80	−4.27	−12.37
His 12δ*	1.53	−0.90	4.25	−1.81	0.91
His 119+*	−1.57	−4.88	6.93	−3.62	−3.90
His 119δ*	2.42	−3.20	8.02	−2.40	−1.40
His 119ε*	2.08	−0.60	3.24	−0.56	0.93
Lys 41+*	−7.52	−0.83	−6.95	0.26	−2.05
Lys 41*	−7.34	3.93	−11.05	−0.23	−0.11
His 12δ* ⇒ His 12+*	−15.35	−14.45	1.55	−2.45	−13.28
His 119δ* ⇒ His 119+*	−3.99	−1.67	−1.09	−1.22	−2.50
His 119ε* ⇒ His 119+*	−3.65	−4.28	3.69	−3.06	−4.83
Lys 41* ⇒ Lys 41+*	−0.17	−4.77	4.10	0.50	−1.94

may not always be justified, as in the case of Lys 41*. The deciding role of the exchange term in this case may be explained by steric effects, because in the R2 structure the methylamine representing Lys 41+ lies close to the protonated OH group of HEMP, which lacks its proton in the PTTS3 structure and can form a hydrogen bond to Lys 41+*. The data for Lys 41* (uncharged) are less relevant because the structure was not optimized after proton extraction; they are presented for comparison only. The results for Lys 41* and His 119* may serve as an example that, even for such evident electrostatic effects as the ionization state of a residue, their impact on the catalytic influence and the physical nature of such a contribution cannot be unambiguously predicted at short distances using simple models. For other residues exerting minor catalytic activity, every term tends to also be important and, because of alternating signs of various contributions, approximations neglecting any one of them may lead to qualitatively incorrect conclusions. On the other hand, the slightly larger distance of His 12* from the reactant (2.4 Å as compared to 1.9 Å for other ligands, Table I) may explain the domination of the electrostatic term, which also seems to be quite well described using simple electrostatic models based on atomic multipole expansion.

A similar analysis performed for the alternative pathway starting from R1 is presented in Table III for His 119*. In this case, the electrostatic influence of ionized His 119+* could be recognized as being responsible for most of the catalytic effect observed, but the effect is rather small, similar to the R2 ⇒ PTTS3 transition. On the contrary, interaction energies of His 119+ with the reactants reach 30 kcal/mol (Table I), so this residue is rather more important for binding of reactants than for stabilization of any of the transition states PTTS1, PTTS2, and PTTS3 over the respective substrates. These results are not contrary to the experimental studies that support the general acid role of His 119, because it acts as an acid at the further reaction stages, which were not investigated here. On the other hand, our results justify the initial protonation state of His 119 as being positive.

A visual comparison of the results presented in Tables II and III is arranged in Figure 4. This diagram shows the data from Tables II and III in relation to the diagram of the relative energetics of the reaction path (Fig. 3). Figure 4 presents the relative lowerings of the activation barriers due to the protonation of different species and may serve to confirm the role of protonation of a catalytic moiety for a specific stage of the reaction in comparison to other residues or structures. The catalytic effects of all three ligands for the R2 ⇒ PTTS3 transition should sum to the height of the overall activation barrier; this was not done for the clarity of the diagram.

The analysis reported so far was performed for very short distances between interacting species, where the short- and long-range contributions are

TABLE III.
Stabilization Energies for First Reaction Stages of Path R1 ⇒ PTTS1 ⇒ I1 ⇒ PTTS2 (Upper Part) and Activation Energy Changes (Lower Part) Resulting from Protonation of Active Site Residue His 119 (kcal/mol).

State Change	$\Delta\Delta E_{res}^{SCF}(D)$	$\Delta E_{el}^{(1)}(D)$	$\Delta E_{ex}^{(1)}(D)$	$\Delta E_{del}^{(R)}(D)$
R1 ⇒ PTTS1				
H119δ*	1.29	0.61	0.81	−0.11
H119+*	4.18	3.68	0.65	−0.15
I1 ⇒ PTTS1				
H119δ*	−1.54	−1.96	1.32	−0.91
H119+*	−4.53	−4.57	1.20	−1.16
I1 ⇒ PTTS2				
H119δ*	−1.31	0.42	−2.24	0.51
H119+*	−5.00	−3.64	−1.94	0.58
R1 ⇒ PTTS1				
H119δ* ⇒ H119+*	+2.90	+3.10	−0.17	−0.04
I1 ⇒ PTTS1				
H119δ* ⇒ H119+*	−2.98	−2.61	−0.12	−0.24
I1 ⇒ PTTS2				
H119δ* ⇒ H119+*	−3.69	−4.06	+0.30	+0.08

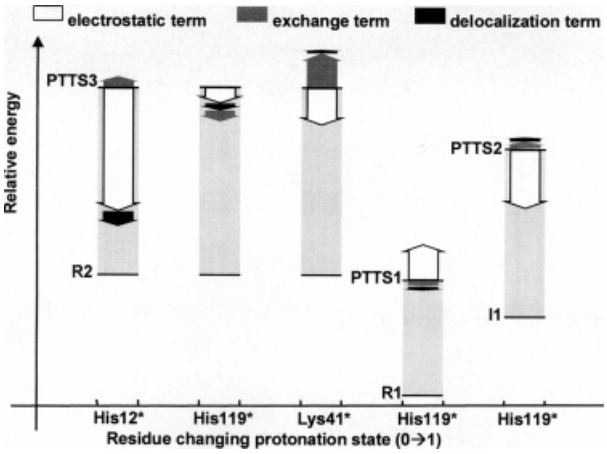

FIGURE 4. The nature of the differential transition state stabilization resulting from protonation of various active site residues. The energy components of the catalytic contributions were calculated as the differences between the respective components of the DTSS energies of protonated and deprotonated forms of the active residues. The relative contributions shown in the diagram sum to the total catalytic effects of protonation of each residue and are compared with the corresponding activation barriers (light gray bars).

frequently comparable. A natural question arises as to at what distance the short-range terms vanish and may be safely neglected. Some results on the distance dependence of various terms of the interaction energy in enzyme models can be found in the literature.[15] Here we want to answer another question. Once we determine an approximate model of long-range interactions (presumably an electrostatic one) and the boundaries within which it may be applied, can we assume that catalytic effects calculated within the scope of our model (i.e., at longer distances) are qualitatively related to exact ones? In order to answer this question in more detail, we examined the distance dependence of all components of interaction energies and transition state stabilization energies between His 119* and the reactants (Fig. 5).

For the His 119* reactant system the distance at which the electrostatic term starts to approximate the total energy of interactions well turned out to be about 2.7 Å (closest contact), which is in good agreement with other studies on hydrogen-bonded systems. In Figure 6 we illustrate the distance dependence of various components of differential stabilization energies of transition states PTTS1, PTTS2, and PTTS3. In most cases the convergence of the electrostatic term to the total stabilization energy is similar to that observed for interaction energies. The divergence at short distances is for some cases not too large, but for the others (stabilization of PTTS2 over I1 and PTTS3 over R2) it shows this may be misleading—a conclusion drawn on the basis of the electrostatic term alone could lead to quantitatively improper prediction of the role of the catalytic residue under investigation. One must also remember that for closely located residues the nature of the catalytic effect can sometimes change dramatically with the distance (Fig. 6d). This implies that one cannot extrapolate catalytic effects calculated at longer distances from the reaction center and make conclusions regarding the influence of the same residue at shorter distances. However, it seems to be completely safe to use the electrostatic approach to evaluate the catalytic effect of residues within the second and further shells of solvation. The safe distance may be different for other molecular environments, and this would require a more systematic study. Our results suggest that the electrostatic term alone is able to provide a quantitative description of interactions starting from about 2.7 Å. Qualitative conclusions could probably be drawn for even shorter contacts, as in the case of His 12* (Tables I, II). More closely located residues should be considered at least *implicitly* via any quantum mechanics/molecular mechanics (QM/MM) or EFP approach.[32]

Because differential stabilization energies and interaction energies both tend to be well approximated by the electrostatic term starting from a distance of 2.7 Å, it might indicate a more general regularity. These results could provide a rule of thumb, which for accurate description of both short-range and long-range interactions using a hybrid approach like QM/MM, any ligand closer to the reaction center than 3 Å should probably be described by a nonempirical approach or at least with an approximation of the exchange $E_{ex}^{(1)}$ and delocalization $E_{del}^{(R)}$ terms.

Approximate Electrostatic Models

Table IV illustrates the accuracy of some electrostatic models in comparison to the exact electrostatic term of interaction energy with first-shell ligands. The MSK is the Merz–Singh–Kollman potential-derived atomic charges.[39] We used the definition of CAMM described in ref. 35, which was shown to well describe the anisotropy of electrostatic charge distribution necessary to supplement electrostatic monopole models of interaction for modeling hydrogen bonds in peptide systems.[40] The CAMM(3) column contains values calculated using

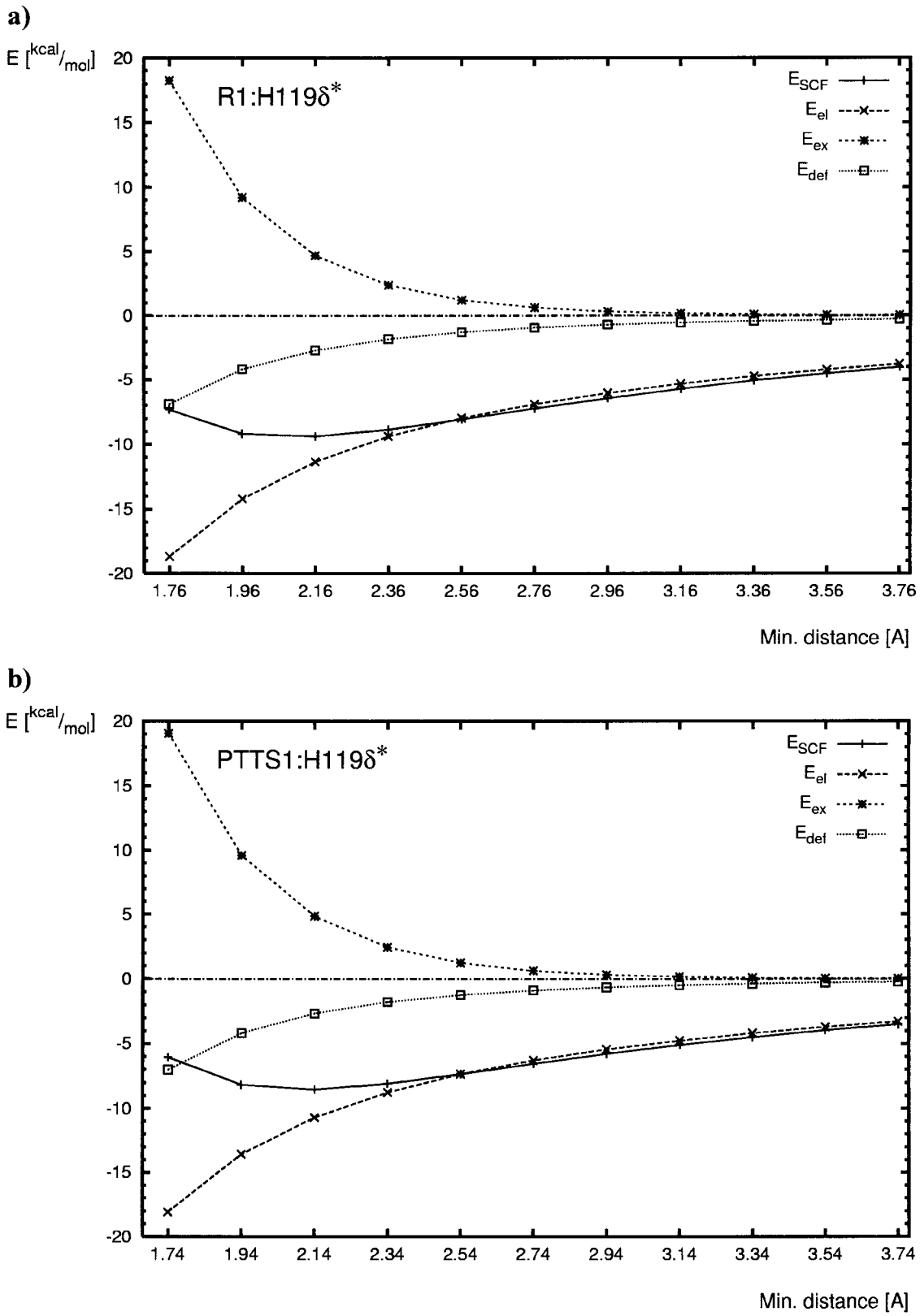

FIGURE 5. The distance dependence of the interaction energy components of His 119δ with stationary point structures on the R1 to PTTS2 pathway: (a) R1-His 119*, (b) PTTS1-His 119*, (c) I1-His 119*, and (d) PTTS2-His 119*. The relevant (native) distances are presented in Figure 2.

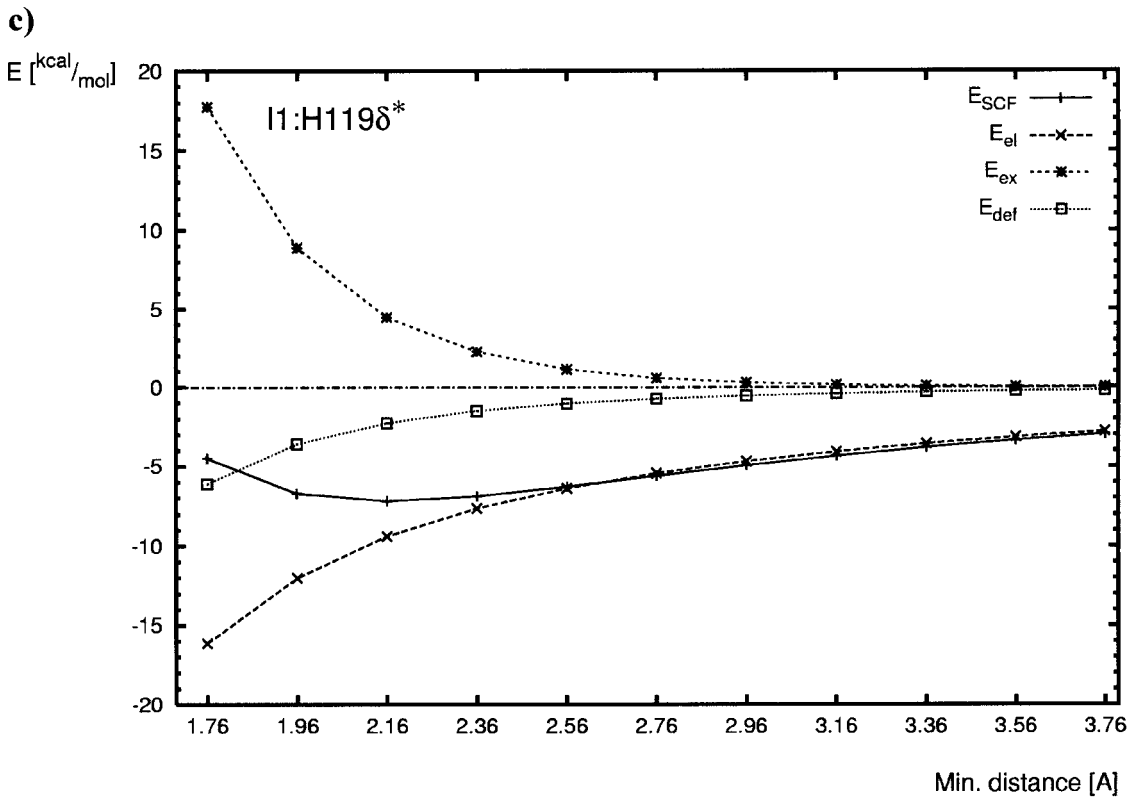

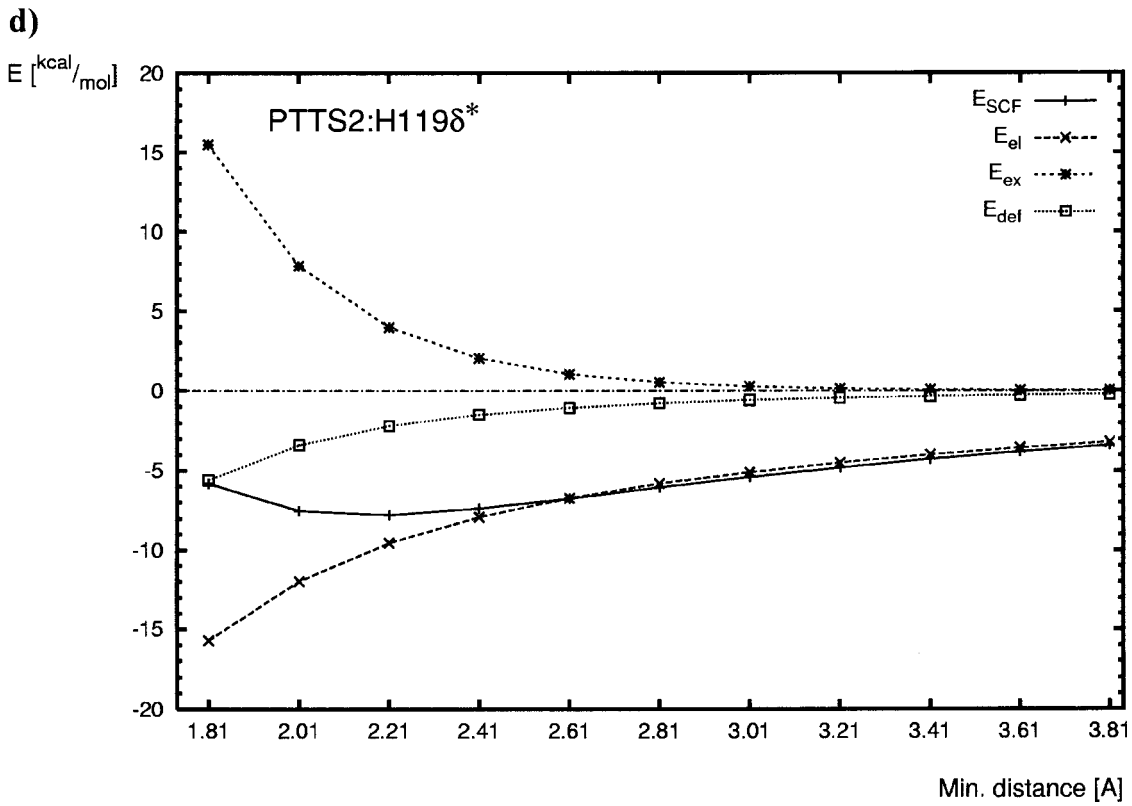

FIGURE 5. (Continued)

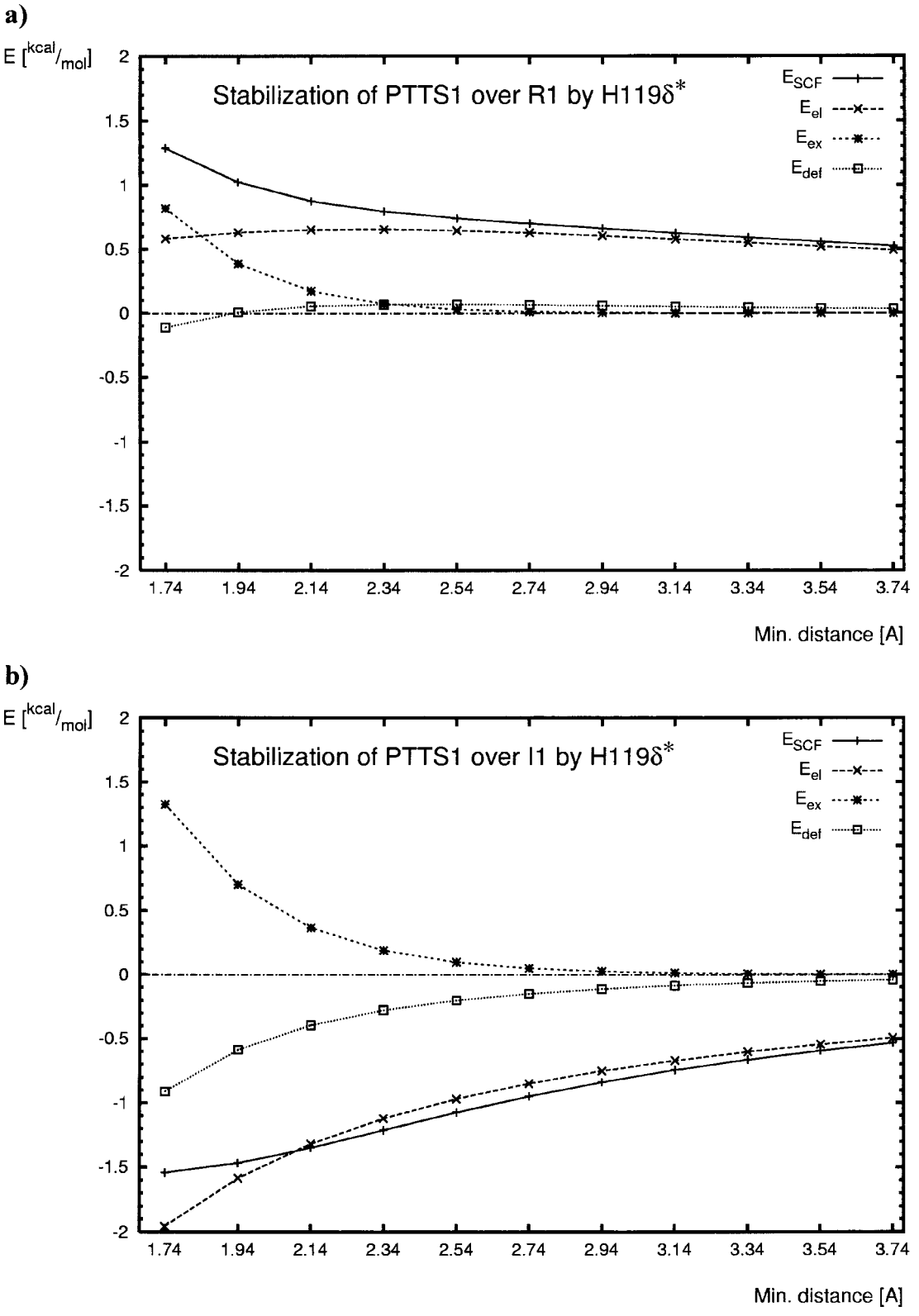

FIGURE 6. The distance dependence of the components of the differential transition state stabilization energy for PTTS1, PTTS2, and PTTS3 transition states of the RNAse A model system. The relevant (native) distances are presented in Figure 2. (a) The stabilization of PTTS1 over R1 by His 119*, (b) stabilization of PTTS1 over I1 by His 119*, (c) stabilization of PTTS3 over R2 by His 119*, and (d) stabilization of PTTS2 over I1 by His 119*.

c)

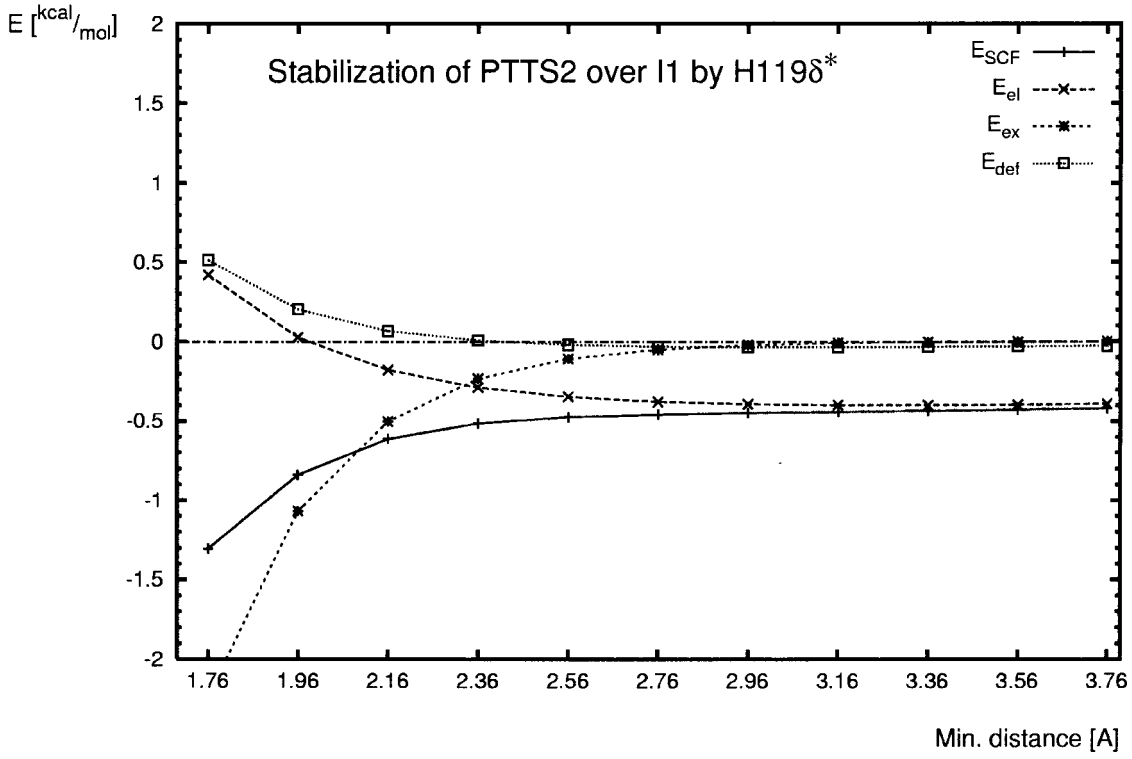

d)

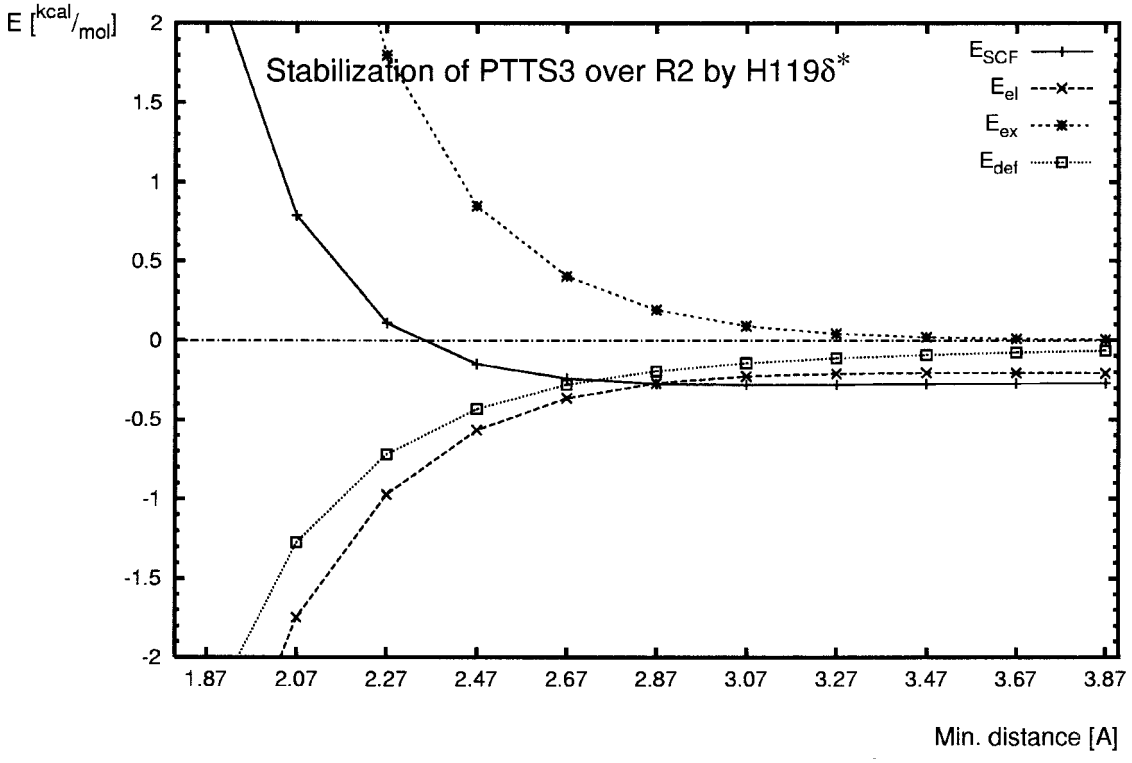

FIGURE 6. (Continued)

TABLE IV.
Comparison of Approximations of First-Order Electrostatic Interaction Energy Terms (kcal/mol).

	Mulliken	MSK	CAMM (3)	CAMM (4)	$\Delta E_{el}^{(1)}$	Shortest Distance (Å)
R1:His 119+*	−34.01	−29.75	32.91	−32.76	−36.35	1.76
R1:His 119δ*	−10.03	−11.66	−14.08	−13.72	−18.67	1.76
R1:His 119ε*	11.46	9.26	10.84	11.21	8.32	2.29
R2:His 119+*	−72.01	−68.48	−69.65	−69.54	−71.36	2.29
R2:His 119δ*	−9.64	−12.65	−13.19	−13.14	−14.81	2.29
R2:His 119ε*	11.37	10.19	11.76	11.52	11.09	2.29
R2:His 12+*	−68.89	−66.43	−67.14	−67.09	−69.97	2.36
R2:His 12δ*	3.12	4.11	3.51	3.83	1.97	2.36
R2:His 12ε*	−7.54	−9.40	−9.74	−9.42	−11.72	2.36
R2:Lys 41+*	−110.04	−107.46	−109.65	−109.28	−116.89	1.70
R2:Lys 41*	−6.60	−11.31	−12.78	−11.12	−23.14	1.70
I1:His 119+*	−25.33	−22.29	−25.57	−25.04	−28.10	1.76
I1:His 119δ*	−8.02	−9.38	−12.03	−11.74	−16.13	1.76
I1:His 119ε*	10.47	8.32	10.00	10.08	7.23	2.30
PTTS1:His 119+*	−29.45	−26.37	−29.79	−29.18	−32.67	1.74
PTTS1:His 119δ*	−9.11	−11.10	−13.67	−13.23	−18.09	1.74
PTTS1:His 119ε*	11.63	9.38	11.21	11.33	8.46	2.29
PTTS2:His 119+*	−29.36	−26.52	−29.38	−28.89	−31.74	1.81
PTTS2:His 119δ*	−8.10	−9.75	−12.03	−11.76	−15.71	1.81
PTTS2:His 119ε*	10.52	8.61	10.15	10.30	7.85	2.28
PTTS3:His 119+*	−76.00	−71.35	−73.85	−73.44	−76.24	1.87
PTTS3:His 119δ*	−10.58	−13.09	−14.78	−14.55	−18.02	1.87
PTTS3:His 119ε*	12.19	10.68	12.28	12.45	10.50	2.31
PTTS3:His 12+*	−81.53	−79.64	−80.24	−79.46	−85.32	1.82
PTTS3:His 12δ*	3.49	5.30	4.81	4.74	1.07	2.35
PTTS3:His 12ε*	−10.36	−13.17	−13.82	−12.59	−17.39	1.82
PTTS3:Lys 41+*	−110.77	−109.90	−113.93	−111.33	−117.72	1.68
PTTS3:Lys 41*	−6.45	−11.03	−13.62	−11.23	−19.20	1.68

a multipole series terminated at the R^{-3} term and CAMM(4) at the R^{-4} term. Because the CAMM series expanded to the R^{-4} term (including octupole moments) is close to convergence, the difference between $E_{el}^{(1)}$ and CAMM(4) energy represents the penetration term of the interaction energy well.

Conclusions

- The same residue may exert a catalytic activity of a different nature, depending on the reaction step.
- When the shortest contacts between reactants and ligands are smaller than about 2.7 Å, none of the interaction energy terms is able to approximate the total energy and none can be neglected.
- For the shortest contact between the reactants and ligand exceeding about 2.7 Å, the electrostatic term converges to the total interaction energy.
- For residues with the shortest contacts with reactants smaller than 2.7 Å, the nature of the catalytic effect can change dramatically with the distance between ligands and qualitative extrapolations to another distance may lead to improper results.

Acknowledgments

Our calculations were carried out at the Wrocław (WCSS), Poznań (PSC), and Warsaw (ICM) Supercomputer Centers.

References

1. Sokalski, W. A. J Mol Catal 1985, 30, 395–410.
2. Warshel, A.; Sussman, F.; Hwang, J. K. J Mol Biol 1988, 201, 139–159.

3. Warshel, A. Computer Modelling of Chemical Reactions in Enzymes and Solutions; Wiley: New York.
4. Perutz, M. F. Faraday Discuss 1992, 93, 111.
5. Náray–Szabó, G.; Warshel, A. Computational Approaches to Biochemical Reactivity; Kluwer: Dordrecht, 1997; Chapter 6.
6. Warshel, A. J Biol Chem 1998, 273, 27035–27038.
7. Kollman, P. A.; Allen, L. C. Theor Chim Acta 1970, 18, 399–403.
8. Morokuma, K. J Chem Phys 1971, 55, 1236–1244.
9. Kitaura, K.; Morokuma, K. Int J Quantum Chem 1976, 10, 325–340.
10. Cammi, R.; Bonaccorsi, R.; Tomasi, J. Theor Chim Acta 1985, 68, 271–283.
11. Szalewicz, K.; Jeziorski, B. In Molecular Interactions, From van der Waals to Strongly Bound Complexes; Scheiner, S., Ed.; Wiley: Chichester, U.K., 1997; Chapter 1.
12. Sokalski, W. A.; Roszak, S.; Pecul, K. Chem Phys Lett 1988, 153, 153–159.
13. Stevens, W. J.; Fink, W. H. Chem Phys Lett 1987, 139, 15–22.
14. Bagus, P. S.; Illas, F. J Chem Phys 1992, 96, 8962–8970.
15. Alagona, G.; Ghio, C.; Monti, S. J Phys Chem A 1998, 102, 6152–6160.
16. Haydock, K.; Lim, C.; Brünger, A. T.; Karplus, M. J Am Chem Soc 1990, 112, 3826–3831.
17. Lim, C.; Karplus, M. J Am Chem Soc 1990, 112, 5872–5873.
18. Dejaegere, A.; Lim, C.; Karplus, M. J Am Chem Soc 1991, 113, 4353–4355.
19. Dejaegere, A.; Karplus, M. J Am Chem Soc 1993, 115, 5316–5317.
20. Dejaegere, A.; Liang, X.; Karplus, M. J Chem Soc Faraday Trans 1994, 90, 1763–1770.
21. Brünger, A. T.; Brooks, C. L.; Karplus, M. Proc Natl Acad Sci USA 1985, 82, 8458–8462.
22. Náray–Szabó, G.; Nagy, J.; Bérces, A. J Mol Struct (Theochem) 1989, 200, 401–412.
23. Glennon, T. M.; Warshel, A. J Am Chem Soc 1998, 120, 10234–10247.
24. Lim, C.; Tole, P. J Am Chem Soc 1992, 114, 7245–7252.
25. Wladkowski, B. D.; Krauss, M.; Stevens, W. J. J Phys Chem 1995, 99, 6273–6276.
26. Wladkowski, B. D.; Krauss, M.; Stevens, W. J. J Am Chem Soc 1995, 117, 10537–10545.
27. Raines, R. T. Chem Rev 1998, 98, 1045–1065.
28. Anslyn, E.; Breslow, R. J Am Chem Soc 1989, 111, 4473–4482.
29. Breslow, R.; Xu, R. Proc Natl Acad Sci USA 1993, 90, 1201–1207.
30. Hershlag, D. J Am Chem Soc 1994, 116, 11631–11635.
31. Gerlt, J. A.; Gassman, P. G. Biochemistry 1993, 32, 11943–11952.
32. Day, P. N.; Jensen, J. H.; Gordon, M. S.; Webb, S. P.; Stevens, W. J.; Krauss, M.; Garmer, D.; Basch, H.; Cohen, D. J Chem Phys 1996, 105, 1968–1986.
33. Roos, B. O. Lecture Notes in Quantum Chemistry; Springer–Verlag: Berlin, 1992; Vol. 58, pp. 177–254.
34. Pauling, L. Chem Eng News 1946, 24, 1375–1377.
35. Sokalski, W. A.; Poirier, R. A. Chem Phys Lett 1983, 98, 86–92.
36. Kędzierski, P.; Sokalski, W. A. unpublished results.
37. Frisch, M. J.; Trucks, G. W.; Schlegel, H. B.; Gill, P. M. W.; Johnson, B. G.; Robb, M. A.; Cheeseman, J. R.; Keith, T.; Petersson, G. A.; Montgomery, J. A.; Raghavachari, K.; Al-Laham, M. A.; Zakrzewski, V. G.; Ortiz, J. V.; Foresman, J. B.; Ciosłowski, J.; Stefanov, B. B.; Nanayakkara, A.; Challacombe, M.; Peng, C. Y.; Ayala, P. Y.; Chen, W.; Wong, M. W.; Andres, J. L.; Replogle, E. S.; Gomperts, R.; Martin, R. L.; Fox, D. J.; Binkley, J. S.; Defrees, D. J.; Baker, J.; Stewart, J. P.; Head–Gordon, M.; Gonzales, C.; Pople, J. A. Gaussian 94, Revision E.2; Gaussian, Inc.: Pittsburgh, PA, 1995.
38. Schmidt, M. W.; Balridge, K. K.; Boatz, J. A.; Elbert, S. T.; Gordon, M. S.; Jensen, J. H.; Koseki, S.; Matsunaga, N.; Nguyen, K. A.; Su, S. J.; Windus, T. L.; Dupuis, M.; Montgomery, J. A. J Comput Chem 1993, 14, 1347–1363.
39. Singh, U. C.; Kollman, P. A. J Comput Chem 1984, 5, 129–145.
40. Sokalski, W. A.; Keller, D. A.; Ornstein, R. L.; Rein, R. J Comput Chem 1993, 14, 970–976.